Int J Earth Sci (Geol Rundsch)
DOI 10.1007/s00531-012-0776-1

ORIGINAL PAPER

Link between global cooling and mammalian transformation across the Eocene–Oligocene boundary in the continental interior of Asia

Rui Zhang · Vadim A. Kravchinsky · Leping Yue

Received: 11 August 2011 / Accepted: 1 April 2012

Abstract Evidence in the world's ocean current system indicates an abrupt cooling from 34.1 to 33.6 Ma across the Eocene–Oligocene boundary at 33.9 Ma. The remarkable cooling period in the ocean, called the Eocene–Oligocene transition (EOT), is correlated with pronounced mammalian faunal replacement as shown in terrestrial fossil records. For the first time within Asia, a section is magnetostratigraphically dated that also produces mammalian fossils that span the Late Eocene—Early Oligocene transition. Three fossil assemblages revealed through the EOT (34.8, 33.7, and 30.4 Ma) demonstrate that perissodactyl faunas were abruptly replaced by rodent/lagomorph-dominant faunas during climate cooling, and that changes in mammalian communities were accelerated by aridification in central Asia. Three fossil assemblages (34.8, 33.7, and 30.4 Ma) within the north Junggar Basin (Burqin section) tied to this magnetostratigraphically dated section, reveal that perissodactyl faunas were abruptly replaced by rodent/lagomorph-dominant faunas during climate cooling, and that changes in mammalian communities were accelerated by aridification in central Asia. The biotic reorganization events described in the Burqin section are comparable to the Grande Coupure in Europe and the Mongolian Remodeling of mammalian communities. That is, the faunal transition was nearly simultaneous all over the world and mirrored global climatic changes with regional factors playing only a secondary role.

Keywords Eocene–Oligocene boundary · Eocene–Oligocene transition · Junggar Basin · Magnetostratigraphy · Paleomagnetism

Introduction

As recorded by a large-scale positive marine benthic $\delta^{18}O$ anomaly and gradual drops in sea level, a dramatic decrease in deep-sea temperature occurred across the Eocene–Oligocene boundary (EOB) 33.9 Ma (Miller et al. 1987; Zachos et al. 2001; Coxall et al. 2005; Tripati et al. 2005). At the same time, the major continental fauna alteration in North America, Europe, and Asia is attributed to the climatic Eocene–Oligocene transition (EOT) (Meng and McKenna 1998; Grimes et al. 2005; Gale et al. 2006; Zanazzi et al. 2007). The global scale climate change during the EOT caused one of the most significant mammal biotic reorganization events since the extinction at the end of the Cretaceous period (Meng and McKenna 1998; Kraatz and Geisler 2010). Eocene–Oligocene land mammalian fossils clearly record this reorganization, termed the Mongolian Remodeling in Asia and the Grande Coupure in Europe, when medium-sized perissodactyl communities

Electronic supplementary material The online version of this article (doi:10.1007/s00531-012-0776-1) contains supplementary material, which is available to authorized users.

R. Zhang · V. A. Kravchinsky (✉)
Department of Physics, University of Alberta, Edmonton, AB T6G 2E1, Canada
e-mail: vadim@ualberta.ca

R. Zhang · L. Yue
State Key Laboratory for Continental Dynamics, Department of Geology, Institute of Cenozoic Geology and Environment, Northwest University, Xi'an 710069, China

L. Yue
State Key Laboratory of Loess and Quaternary Geology, Institute of Earth Environment, Chinese Academy of Sciences, Xi'an 710075, China

Published online: 21 May 2012

were abruptly replaced by small-sized rodent/lagomorph-dominant faunas (Meng and McKenna 1998; Kraatz and Geisler 2010; Costa et al. 2011). The age of the Mongolian Remodeling, however, is still not precisely reconstructed.

A broad pattern of aridification across the late Eocene and early Oligocene epochs within central Asia was recently reported in Mongolia (Kraatz and Geisler 2010) and the northeast Tibetan Plateau (Dai et al. 2006; Dupont-Nivet et al. 2007, 2008). Dupont-Nivet et al. (2007, 2008) and Abels et al. (2011) built an age model based on magnetostratigraphy and correlations between local/regional pollen records and a marine oxygen isotope reference curve to perform their paleoenvironmental reconstructions in the Xining Basin of northeastern Tibet. The mammalian fossils found in the upper part of the Tibetan section correspond to the late Oligocene. Dai et al. (2006) demonstrated that late Eocene to early Oligocene fossils were missing in Xining. Therefore, other studies are required in order to find a section with both late Eocene and early Oligocene fossils and to clarify the timing of the EOT in Asia. Kraatz and Geisler (2010) reported on several sections across the EOT from Mongolia. Their age model was based on a magnetostratigraphic compilation and direct tie points to the geomagnetic polarity time scale (GPTS) via radioisotopically dated basalts for a few short sedimentary sequences that sometimes contained only one or two normal/reversed polarity zones. Although the authors described faunal transitions during the EOT, late Eocene faunas were not found. Finding both late Oligocene and early Eocene faunas in one section would confirm the timing of the EOT and determine the upper/lower limits of the transition in continental Asia.

To better understand the character and timing of the faunal transformation in Asia compared to Europe, as well as differences and similarities between continental and oceanic climate changes around the Eocene–Oligocene boundary, we studied the Burqin section (northern Junggar Basin, central Asia). The section is situated 1,000 km to the west of the Mongolian section described by Kraatz and Geisler (2010). Our section could be compared to sections from similar time intervals in Europe and Mongolia in order to specify a linkage to faunal transformation during the EOT (Wu et al. 2004; Ye et al. 2005; Ni et al. 2007; Costa et al. 2011).

The Junggar Basin, formed during late Paleozoic, Mesozoic, and Cenozoic, is a large-scale piled sedimentary basin bounded by the Tian-Shan Mountains to the south and the Altay Mountains to the north. Bosboom et al. (2011) demonstrate the remnants of a large epicontinental sea at the end of Eocene in the middle of the Asian continent. In this paper, we base the timing of terrestrial cooling and aridification on our magnetostratigraphic dating of mammalian fauna findings in the Burqin section.

Mammalian fossils of the Burqin section

The terrestrial Tertiary strata on the northern bank of the Irtysh River near Burqin City (Fig. 1) consist of lower rusty-yellow and purplish red beds of the Irtysh River Formation, and upper yellowish-green sandstones with variegated green mudstones beds of the Keziletuogayi Formation (Ye et al. 2005; Ni et al. 2007). All stratigraphic layers in the northern part of the Junggar Basin are horizontal, and there are no signs of sedimentary discontinuities or tectonic deformations in the region that makes the Burqin section one of the key sections to study the EOT in Asia. The sedimentary strata are folded and steep only in the southern periphery of the basin (Carroll et al. 1990).

Three mammalian fossil assemblages were found across the EOB during 1998 to 2006 within the Keziletuogayi Formation in the Burqin section (Wu et al. 2004; Ye et al.

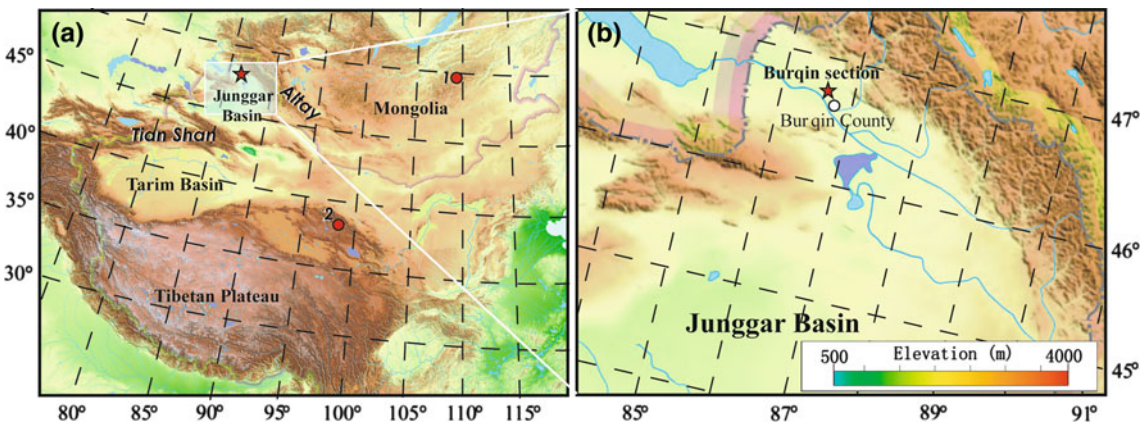

Fig. 1 **a** Study area location in Asia. **b** Location of the Junggar Basin and the Burqin section. The key Eocene–Oligocene localities in Asia: *1* Mongolia (Kraatz and Geisler 2010); *2* Xining Basin (Dai et al. 2006; Dupont-Nivet et al. 2007, 2008). Our study area is marked as a *star*

2005; Ni et al. 2007). The first assemblage was discovered in a 70-mm thin layer of black manganese siltstone in grayish green mudstone at a depth of 58 m. These findings are described in detail by Ye et al. (2005) and Ni et al. (2007) (see Table 1 in Ni et al. (2007) and Figure SM-1 in the online Supplementary Materials). The first assemblage is similar to the Khoer-Dzan and Ergilin faunas of Mongolia (Wu et al. 2004; Ye et al. 2005; Ni et al. 2007). Six species representing four families include *Cadurcodon* cf. C. *ardynensis*, Amynodontidae gen. et sp. indet., *Gigantamynodon giganteus*, Indricotheriinae gen. et sp. indet., Rhinocerotidae gen. et sp. indet., and Brontotheriidae gen. et sp. indet.; all are perissodactyls. There were no fossils of small mammals found in the paleontological screen-washing. The apparent lack of forest-related species like euprimates, chiropterans, and plesiadapiformes suggests an absence of dense forest in Burqin during the studied interval. *Rhynchosia* and *Elaeagnus* pollen findings and evidence of perissodactyl-dominant mammals indicate a warm subtropical climate (Ye et al. 2005).

The second mammalian assemblage includes fossils found at a depth of 45 m in a 1.7 m layer of brown mudstone in between green sandstone strata (Fig. 2) (Ye et al. 2005; Ni et al. 2007). Fossils collected from the Burqin section and two other neighboring localities of the same stratigraphic level represent 13 species from 7 mammalian genera (see Table 1 in Ni et al. (2007) for the complete listing); all are mammals similar in size to *Hyaenodon* sp. and *Desmatolagus* sp. and comparable to early Shandgolian faunas (Ye et al. 2005; Ni et al. 2007) (also spelled as Hsandagolian faunas in literature). The perissodactyl components entirely disappear in the second mammalian fossil assemblage. Such a critical change in the mammalian assemblage indicates a faunal transformation from perissodactyl-dominant mammals to rodents and lagomorphs within the section.

The third assemblage, collected at a depth of 65 m in green mudstone, is similar to the second, but importantly reflects a faunal change from the lower two assemblages. The dominant small-sized mammals of the third assemblage included 16 species similar in size to *Palaeoscaptor* cf. *P. acridens* and *Tupaiodon* cf. *T. morrisi*, and analogous to the Shandgolian from Mongolia (Meng and McKenna 1998; Ye et al. 2005; Kraatz and Geisler 2010).

The faunas transition in the Burqin basin correspond to the Mongolian Remodeling and the Grande Coupure from Europe (Meng and McKenna 1998; Wu et al. 2004; Ye et al. 2005; Ni et al. 2007) linking those areas to the same global cooling event across the Eocene–Oligocene boundary. In all of these sections, Late Eocene faunas were dominated by large perissodactyls, whereas the Early Oligocene faunas are rich in rodents and lagomorphs.

The magnetostratigraphic result

In the Burqin section, we were able to sample a 128 m interval that corresponds to the Irtysh River (lower part of the section) and Keziletuogayi (upper part of the section) formations at the north bank of the Irtysh River. Paleomagnetic sampling was performed approximately every 0.5 m. The paleomagnetic fold test could not be applicable because of the horizontal bedding orientation. The uppermost stratum of the section was dominated by a massive grayish-white fluvial conglomerate that made paleomagnetic sampling unfeasible. Therefore, our sampling began from the grayish lacustrine sandstone and mudstone layers beneath the conglomerate layer. There was a general trend toward coarser particles upward to the top of the section. At a depth of 26–37 m, the lithology of the Keziletuogayi Formation was dominated by coarse yellowish sandstone, which also did not yield to paleomagnetic analysis.

We performed measurements of magnetic susceptibility (MS or χ) versus temperature (χ-T curves) of the bulk sediment using an AGICO KLY-3 Kappabridge susceptibility meter coupled with a CS-3 high-temperature furnace,

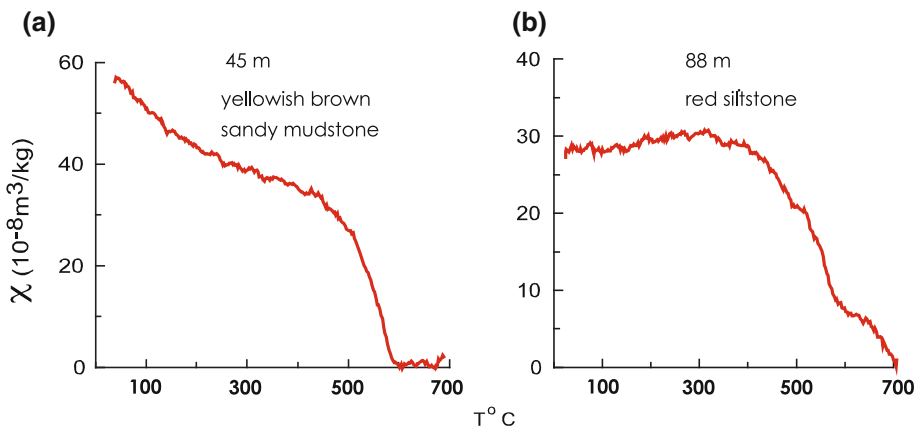

Fig. 2 Temperature dependence of magnetic susceptibility for representative samples from the Burqin section

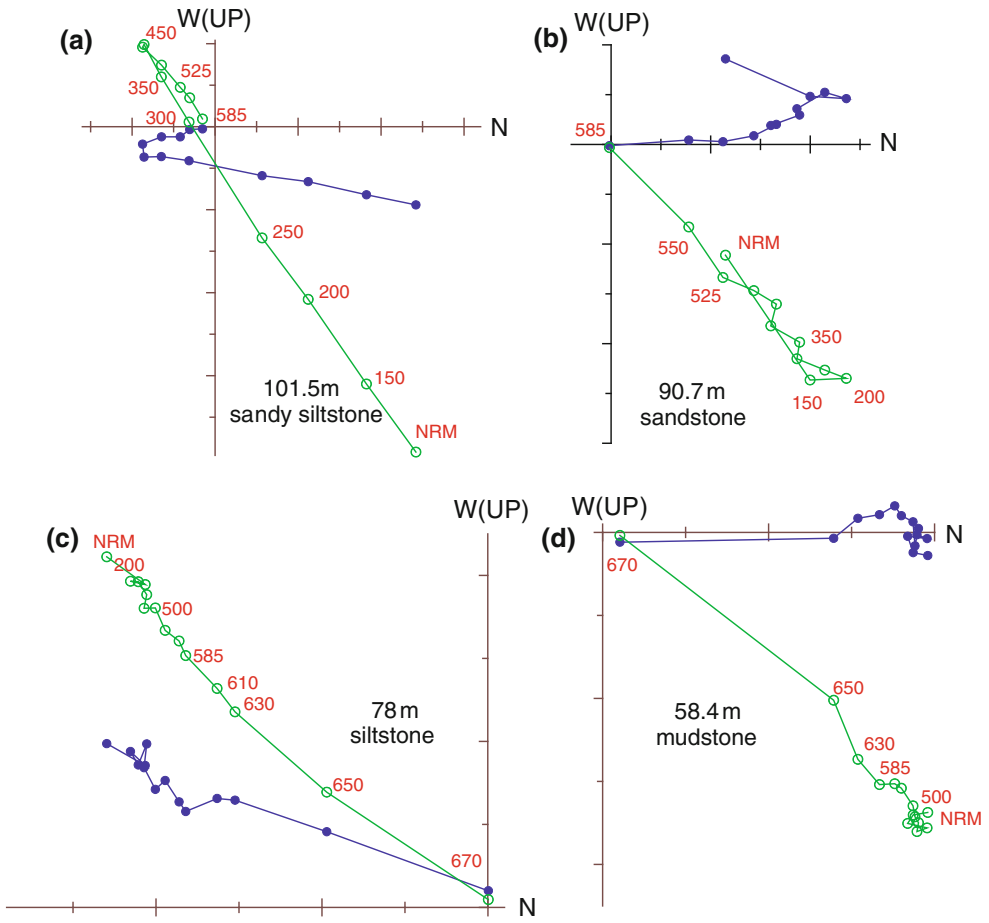

Fig. 3 Representative orthogonal vector projections of stepwise thermal demagnetization of natural remanent magnetization for the Burqin section. Demagnetization steps are in °C for all plots; *open and solid circles* represent vector endpoints projected onto vertical and horizontal planes, respectively

from room temperature to 700 °C in an argon atmosphere to prevent oxidation during heating. As shown in Fig. 2, the χ-T curves usually can be divided into two categories according to their Curie-temperature behavior. The Type I curve (Fig. 2a) represents the MS of brown sandstones or sandy mudstones and demonstrates a characteristic decline in magnetic susceptibility from 450 to 585 °C, a characteristic of sediment containing magnetite. A moderate decrease in MS below 200 °C is caused by contributions of paramagnetic minerals following the Curie–Weiss law. The Type II curve (Fig. 2b) represents the MS of red siltstones and mudstones. The curve demonstrates two critical decreases in MS at 585 and 690 °C, indicating that magnetite and hematite are major contributors.

Magnetic remanence was measured with a 2-G, three-axis, cryogenic magnetometer housed inside a magnetic shield with a background magnetic field of less than 300 nT. In the laboratory, we thermally demagnetized 178 samples from different depth intervals, applying 12–16 temperature steps up to 690 °C and measured the natural remanent magnetization (NRM) after every step. Representative orthogonal vectors diagrams demonstrate that the studied samples possess two magnetic components. The low-temperature component (LTC) does not decay toward the original and usually could be removed at 250 °C (Fig. 3b–d). In a few samples, the LTC was removed at 450 °C (Fig. 3a). The high-temperature component (HTC) was observed from 300 to 585 °C in greystones and to 690 °C in redstones and always decayed toward the origin on the orthogonal diagrams. The same HTC direction in gray and red beds with magnetite and hematite, respectively, as the carriers of magnetization is defined as the characteristic remanent magnetization (ChRM) direction.

Our paleomagnetic analyses yielded reliable ChRM directions from 126 samples. We identified 11 normal polarity and 11 reversed polarity intervals. The detailed magnetostratigraphy was determined by declination and inclination correlations to the geomagnetic polarity time scale of Cande and Kent (1995). In the Burqin section, 96 stable HTC directions were selected for the calculation of the mean paleomagnetic direction: declination $D = 359.6°$,

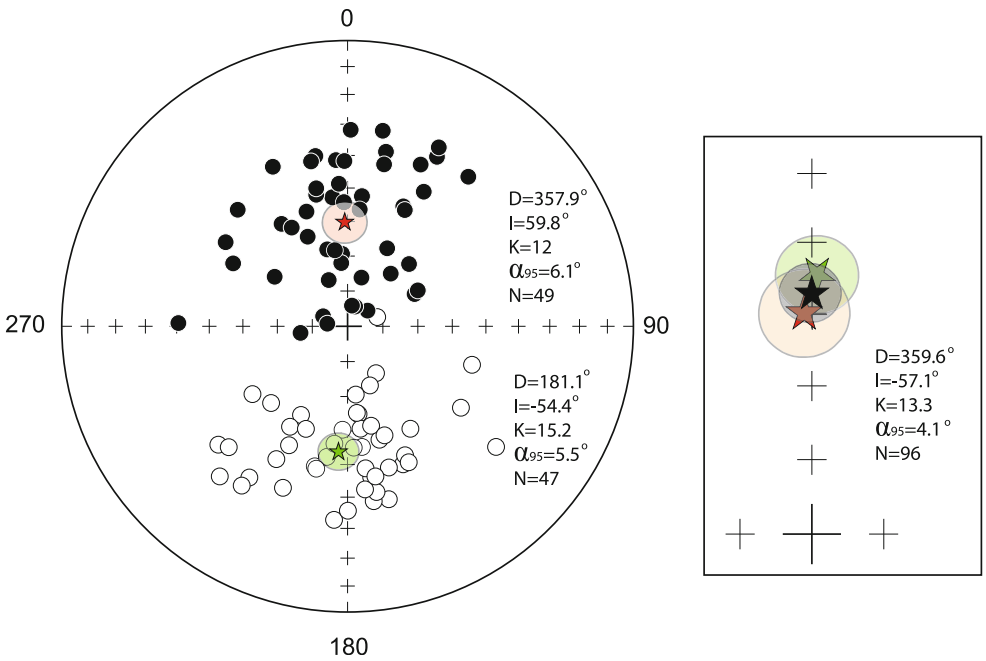

Fig. 4 Equal area projection of the high-temperature component directions for 96 stable samples in the Burqin locality (plotted using PaleoMac software (Cogné 2003). *Closed* (*open*) *symbols*: downward (upward) inclinations. A *red* (*green*) *star* represents the mean direction for the normal (reverse) polarity based on its α_{95} circle of confidence. *Black star* represents the mean direction of the section with its corresponding α_{95} circle of confidence

inclination $I = 57.1°$, $k = 13.3$, and $\alpha_{95} = 4.1°$ (precision parameter and half-angle radius of the 95 % probability confidence cone). The presence of two opposite polarity directions yields a positive reversal test (class B, following the classification of McFadden and McElhinny 1990) (Fig. 4). At 95 % confidence, the difference between normal (N) and reverse (R) polarities is 5.7° ($D_N = 0.1°$, $I_N = 64.4°$, $k = 12.0$, $\alpha_{95} = 7.7°$, $N = 53$ samples; $D_R = 181.7°$, $I_R = 55.5°$, $k = 15.2$, $\alpha_{95} = 6°$, $N = 43$ samples), which is less than the critical angle $\gamma_c = 8.2°$.

Paleontological constraints show that perissodactyls dominate faunas of the Late Eocene, and that rodents and lagomorphs (second and third assemblages in our section) are the dominant faunas of the Early Oligocene. In the context of our study, this suggests that the Eocene–Oligocene boundary is between the first and second assemblages of the Burqin section (Wu et al. 2004; Ye et al. 2005; Ni et al. 2007). We matched our polarity scale to the GPTS in the most evident intervals of reverse polarity at 40–55 m, R2 and R3, to the long reverse polarity chrons C13r and C15r, separated by a shorter normal polarity chron C15n (Fig. 5). We then matched other polarity intervals further up and down the section (Table 1). Although alternative models for correlation to the GPTS exist (see below), our model in Fig. 5 provides the most reasonable fit that is in agreement with (1) the mammalian fossil assemblages of the Keziletuogayi Formation found in the section and (2) the gradual increase in sedimentary grain size from fine grain sediment at the bottom of the Burqin section to medium and course sandstone at the top of the section [the rate of sedimentation increased from 0.78 to 0.95 cm/kyr (Fig. 6)].

Linear interpolation between the magnetic chrons yields ages of 34.8 and 33.7 Ma, respectively, for the first and second faunal assemblages (Fig. 5). The third assemblage is right above the N1 normal polarity of our sequences and corresponds to an age of 30.4 Ma.

The alternative magnetostratigraphic model (Figure SM-2 in the online Supplementary Materials) was rejected because it unreasonably shifts the Burqin faunal transition far upward in the studied cross-section. In the rejected model, the transition does not correspond to the EOB and marine oxygen isotope curve transition. The model would also imply the sedimentation rate decreases from 0.78 to 0.56 cm/kyr around the central segment of the studied section and then sharply increases again to the top of the section. It contradicts the field observation of the gradual increase in the sedimentary grain size at the central part of the cross-section.

Discussion

The fossil assemblages from the Burqin section provide paleontological evidence for the onset of important environmental change across the EOT that is consistent with

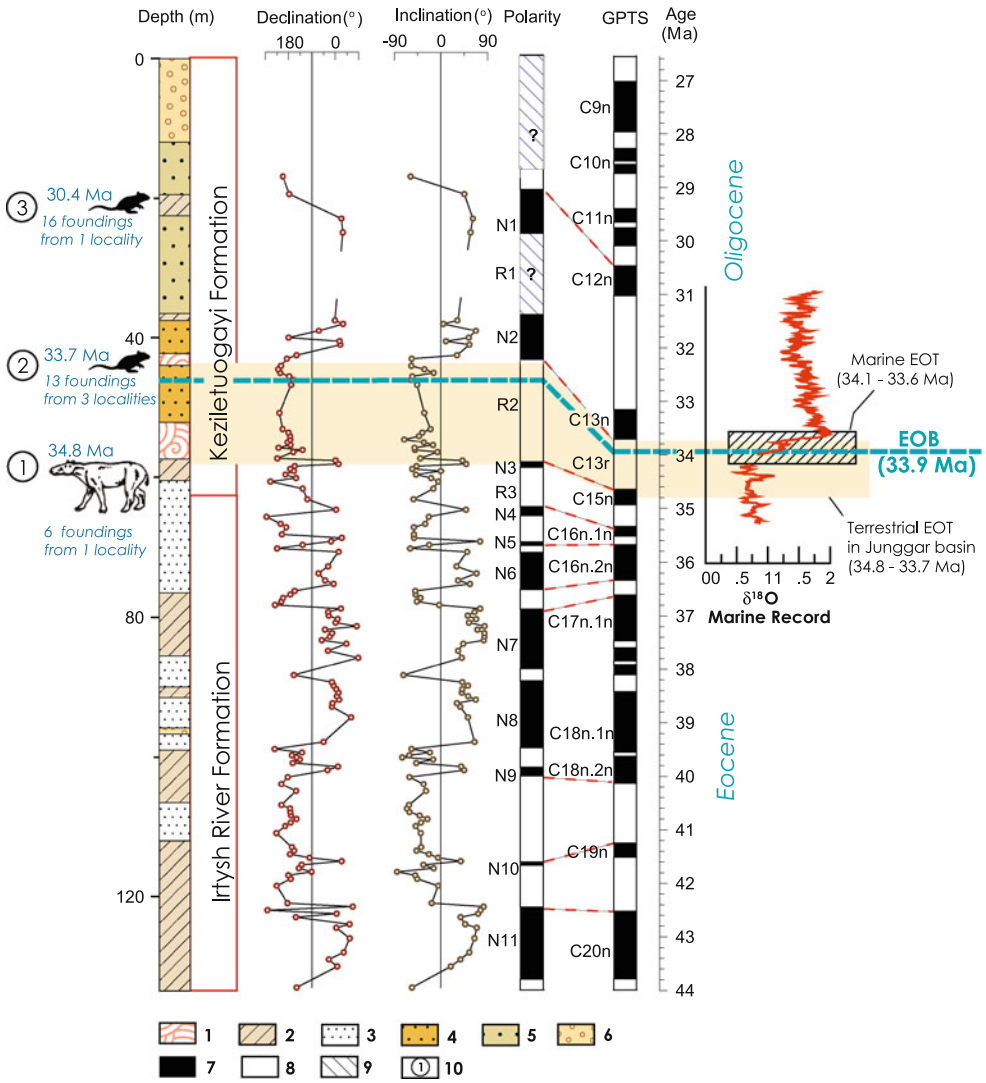

Fig. 5 Detailed magnetostratigraphy of the studied section and its correlation with the GPTS of Cande and Kent (1995). The EOB is at 33.9 Ma (Gradstein et al. 2004). Marine oxygen isotope curve from Coxall et al. (2005). The terrestrial EOT in the Junggar Basin is constructed in this study. *Numbers in the circles* denote the faunal assemblage 1, 2 and 3. *1* mudstone, *2* siltstone, *3* fine sandstone, *4* intermediate size sandstone, *5* coarse sandstone, *6* conglomerate, *7* normal polarity interval, *8* reversed polarity, *9* uncertain polarity, *10* faunal assemblage number after Ni et al. (2007), perissodactyl-dominant mammalian fossils compose the assemblage 1, and rodent/lagomorph-dominant fossils compose the assemblages 2 and 3

the global climate shift characterized by a gradual decrease in deep-sea temperature (Coxall et al. 2005; Tripati et al. 2005) recorded in the marine oxygen isotope curve (Fig. 5). The prominent terrestrial biotic reorganization in central Asia has been recognized and named the Mongolian Remodeling (Meng and McKenna 1998). The Mongolian Remodeling is characterized by a shift from Eocene perissodactyl-dominant faunas to Oligocene rodent/lagomorph-dominant faunas. Recently, Kraatz and Geisler (2010) demonstrated that the first post-Mongolian Remodeling faunas appeared as Hsandagolian EALMA found in the Hsanda Gol Formation in Mongolia at 33.3 Ma. The earliest rodent/lagomorph-dominant fauna in our section was found at 33.7 Ma (Fig. 5), indicating that these faunas could have appeared throughout central Asia at least 0.4 Myr earlier than was previously suggested (Kraatz and Geisler 2010).

Dupont-Nivet et al. (2007) demonstrated that the aridification in central Asia around the EOB was a result of global climatic cooling. The major Tibetan uplift occurred a little earlier (~38 Ma) based on the Xining Basin data (Dupont-Nivet et al. 2008). Gravel stratum in the upper part of the study section indicates a larger river input to the ancient lake (or intracontinental sea area) at the Burqin site at ~30 Ma. The courser grain horizons could indicate the Central Asian epicontinental sea retreat around EOT as discussed by Bosboom et al. (2011). While we observe sedimentation rate changes precisely at the EOB, the

Table 1 Magnetostratigraphic age model for the Burqin section

Depth (m)	Polarity chron intervals (Ma)	Polarity chron nomenclature
19.50	30.479	C12n end
44.25	33.545	C13n
58.35	34.655	C15n end
59.20	34.940	C15n
64.75	35.343	C16n.1n end
66.00	35.526	C16n.1n
69.75	35.685	C16n.2n end
76.50	36.341	C16n.2n
79.25	36.618	C17n.1n end
99.00	39.552	C18n.1n
101.75	39.631	C18n.2n end
103.00	40.130	C18n.2n
115.25	41.257	C19n end
115.75	41.521	C19n
121.75	42.536	C20n end
132.00	43.789	C20n

Correlation was performed using the GPTS of Cande and Kent (1995)

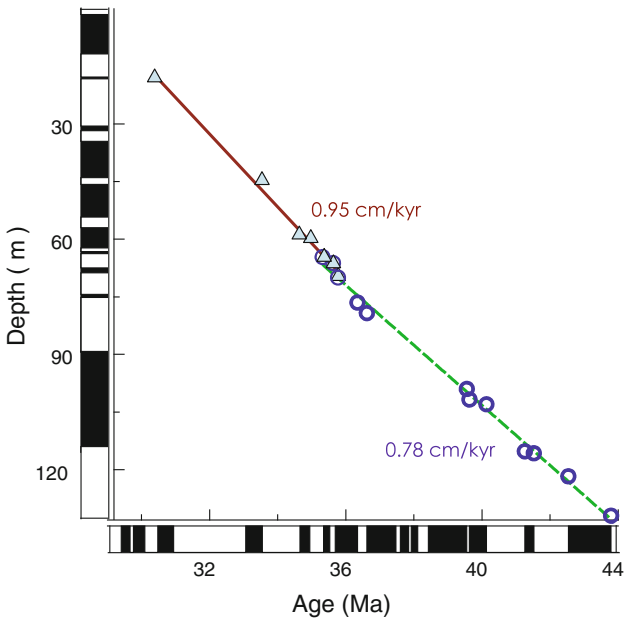

Fig. 6 Stratigraphic level in meters versus age according to magnetostratigraphic correlation with the GPTS in the Burqin section. Sedimentation rates of 0.78 and 0.95 cm/kyr are shown near fine grain (*dashed line*) and coarser grain (*solid line*) sediment intervals in the section. *Circles* (*triangles*) correspond to the geomagnetic event boundaries from Fig. 5 for the fine (*coarser*) grain sediments

mechanism that drove this is unclear as the region was concurrently undergoing major tectonic uplift, climatic change, and sedimentological regime change; all of which are themselves closely intertwined. Regardless of the mechanism, however, it is clear that the sedimentation rate change we observe is strongly correlated temporally to both regional and global events of the Eocene–Oligocene Transition.

Most importantly, our studies imply that mammalian reorganization occurred as a result of global cooling and Asian aridification as shown by Dupont-Nivet et al. (2007).

The uplift of the Tibetan Plateau and the retreat of the Paratethys epicontinental sea triggered aridification of continental Asia (Graham et al. 2005; Harris 2006; Rowley and Currie 2006; Zhang et al. 2007; Dupont-Nivet et al. 2007, 2008), which occurred 3 Myr before the EOB (Dupont-Nivet et al. 2008). Therefore, global cooling may have driven faunal turnover observed during the EOT within Asia. Faunal reorganization within the Junggar Basin occurred quickly, most likely between 34.8 and 33.7 Ma, and was followed by a long period of faunal stability. Such terrestrial faunal change matches overall patterns of reorganization during the marine EOT (34.1–33.6 Ma), both of which were nearly coincident with the EOB (33.9 Ma) (Coxall et al. 2005). It is possible that the terrestrial EOT in the Junggar Basin could have terminated (33.7 Ma) slightly before the onset of the marine EOT (33.6 Ma) and the Grande Coupure in Europe (Costa et al. 2011).

Conclusions

Three fossil assemblages revealed in the Burqin locality (34.8, 33.7, and 30.4 Ma) demonstrate that perissodactyl faunas were abruptly replaced by rodent/lagomorph-dominant faunas. Our study establishes the age of fauna transformations across the Eocene–Oligocene boundary (33.9 Ma) in central Asia for the first time. The Eocene–Oligocene transition in central Asia occurred at nearly the same time as it occurred in Mongolia (Kraatz and Geisler 2010) and Tibet (Dupont-Nivet et al. 2007, 2008). These findings strongly suggest that global cooling played a leading role in the aridification and faunal transformation in Asia.

Acknowledgments We thank Drs. Jin Meng (American Museum of Natural History), Jie Ye, Wenyu Wu, Xijun Ni, Bin Bai (Institute of Vertebrate Paleontology and Paleoanthropology, Chinese Academy of Sciences), Shundong Bi (Indiana University of Pennsylvania), and Jianqi Wang (Northwest University, Xi'an) for their valuable help during the fieldwork. We thank Dr. Brian Kraatz and Dr. Thomas Martin for providing their constructive comments that led to substantial improvement of our manuscript. We thank Marcia Craig for her editing of the text before our submission to the journal. The study was partially funded by the Natural Sciences and Engineering Research Council of Canada's support of V.A.K. Measurements were funded through support for V.A.K. by the Canadian Foundation for Innovation and the University of Alberta and for L.Y. by the National Natural Science Foundation of China (grant 41072136).

References

Abels HA, Dupont-Nivet G, Xiao G, Bosboom R, Krijgsman W (2011) Step-wise change of Asian interior climate preceding the Eocene–Oligocene transition (EOT). Palaeogeogr Palaeoclimatol Palaeoecol 299:399–412

Bosboom RE, Dupont-Nivet G, Houben AJP, Brinkhuis H, Villa G, Mandic O, Stoica M, Zachariasse WJ, Guo ZJ, Li CX, Krijgsman W (2011) Late Eocene sea retreat from the Tarim Basin (west China) and concomitant Asian paleoenvironmental change. Palaeogeogr Palaeoclimatol Palaeoecol 299:385–398

Cande SC, Kent DV (1995) Revised calibration of the geomagnetic polarity time scale for the Late Cretaceous and Cenozoic. J Geophys Res 100:6093–6095

Carroll A, Liang Y, Graham S, Xiao XC, Hendrix M, Chu WM, McKnight C (1990) Junggar basin, northwest China: trapped late Paleozoic ocean. Tectonophysics 181:1–14

Cogné JP (2003) PaleoMac: a MacintoshTM application for treating paleomagnetic data and making plate reconstructions. Geochem Geophys Geosyst 4:1007. doi:10.1029/2001GC000227

Costa E, Garcés M, Sáez A, Cabrera L, López-Blanco M (2011) The age of the "Grande Coupure" mammal turnover: new constraints from the Eocene–Oligocene record of the Eastern Ebro Basin (NE Spain). Palaeogeogr Palaeoclimatol Palaeoecolo 301: 97–107

Coxall HK, Wilson PA, Palike H, Lear CH, Backman J (2005) Rapid stepwise onset of Antarctic glaciation and deeper calcite compensation in the Pacific Ocean. Nature 433:53–57

Dai S, Fang X, Dupont-Nivet G, Song C, Gao J, Krijgsman W, Langereis C, Zhang W (2006) Magnetostratigraphy of Cenozoic sediments from the Xining Basin: tectonic implications for the northeastern Tibetan Plateau. J Geophys Res 111:B11102. doi: 10.129/2005JB004187

Dupont-Nivet G, Krijgsman W, Langereis CG, Abels HA, Dai S, Fang X (2007) Tibetan plateau aridification linked to global cooling at the Eocene–Oligocene transition. Nature 445:635–638

Dupont-Nivet G, Hoorn C, Konert M (2008) Tibtan uplift prior to the Eocene-Oligocene climate transition: evidence from pollen analysis of the Xining Basin. Geology 36:987–990

Gale AS, Huggett JM, Pälike H, Laurie E, Hailwood EA, Hardenbol J (2006) Correlation of Eocene–Oligocene marine and continental records: orbital cyclicity, magnetostratigraphy and sequence stratigraphy of the Solent Group, Isle of Wight, UK. Geol Soc Lond J 163:401–415

Gradstein FM, Ogg JG, Smith AG (2004) A geologic time scale 2004. Cambridge University Press, Cambridge

Graham ST, Chamberlain CP, Yue Y, Ritts BD, Hanson AD, Horton TW, Waldbauer JR, Poage MA, Feng X (2005) Stable isotope records of Cenozoic climate and topography, Tibetan Plateau and Tarim Basin. Am J Sci 305:101–118

Grimes ST, Hooker JJ, Collinson ME, Mattey DP (2005) Temperatures of the late Eocene to early Oligocene freshwaters. Geology 39:189–192

Harris NBW (2006) The elevation history of the Tibetan Plateau and its implications for the Asian monsoon. Palaeogeogr Palaeoclimatol Palaeoecol 241:4–15

Kraatz BP, Geisler JH (2010) Eocene-Oligocene transition in Central Asia and its effects on mammalian evolution. Geology 38: 111–114

McFadden PL, McElhinny MW (1990) Classification of the reversal test in paleomagnetism. Geophys J Int 103:725–729

Meng J, McKenna MC (1998) Faunal turnovers of Paleogene mammals from the Mongolian plateau. Nature 394:364–367

Miller KG, Fairbanks RG, Mountain GS (1987) Tertiary oxygen isotope synthesis, sea level history, and continental margin erosion. Paleoceanography 2:1–19

Ni XJ, Meng J, Ye J, Wu WY (2007) A new Early Oligocene peradectine marsupial (Mammalia) from the Burqin region of Xinjiang, China. Naturwissenschaften 94:237–241

Rowley DB, Currie BS (2006) Palaeoaltimetry of the late Eocene to Miocene Lunpola basin, central Tibet. Nature 439:677–681

Tripati A, Backman J, Elderfield H, Ferretti P (2005) Eocene bipolar glaciation associated with global carbon cycle changes. Nature 436:341–346

Wu W, Meng J, Ye J, Ni X (2004) *Propalaeocastor* (Rodentia, Mammalia) from the early Oligocene of Burqin Basin, Xinjiang. Am Mus Novit 3461:1–16

Ye J, Meng J, Wu W, Ni X (2005) Lithological and biostratigraphic sequence across the Eocene-Oligocene boundary in Burqin of Xinjiang. Vertebrata PalAsiatica 43:49–60

Zachos JC, Pagani M, Sloan L, Thomas E, Billups K (2001) Trends, rhythms, and aberrations in global climate 65 Ma to present. Science 292:686–693

Zanazzi A, Kohn MJ, MacFadden BJ, Terry DO Jr (2007) Large temperature drop across the Eocene–Oligocene transition in central North America. Nature 445:639–642

Zhang Z, Wang H, Guo Z, Jiang D (2007) What triggers the transition of palaeoenvironmental patterns in China, the Tibetan Plateau uplift or the Paratethys Sea retreat? Palaeogeogr Palaeoclimatol Palaeoecol 245:317–331